

Origin of complex crystal structures of elements at pressure

G.J.Ackland, I.R.Macleod and O.Degtyareva

*School of Physics and Centre for Science at Extreme Conditions,
The University of Edinburgh, Mayfield Road, Edinburgh, EH9 3JZ, UK.*

(Dated: October 29, 2018)

We present a unifying theory for the observed complex structures of the sp-bonded elements under pressure based on nearly free electron picture (NFE). In the intermediate pressure regime the dominant contribution to crystal structure arises from Fermi-surface Brillouin zone (FSBZ) interactions - structures which allow this are favoured. This simple theory explains the observed crystal structures, transport properties, the evolution of internal and unit cell parameters with pressure. We illustrate it with experimental data for these elements and ab initio calculation for Li.

PACS numbers: 61.50.Ks,62.50.+p

Recent experimental high-pressure investigations of metallic elements have yielded surprising and intriguing results, with decreasing coordination and increasing crystal complexity at intermediate pressures (fig.1). This behavior can be reproduced by ab initio calculations based on the density functional plane wave pseudopotential method (DFPP) which represents a sufficient theoretical understanding of the problem: there is no need for physics “beyond” DFPP, as is required in the *f*-metal localisation transitions. However, DFPP calculations are sufficiently complex that no simpler theoretical principles emerge. Moreover DFPP calculations require plausible candidate structures - in simple cases picking the “usual suspects” and symmetry-breaking distortions therefrom has worked, but when very complex structures are contenders, a more systematic approach is needed. Here, we demonstrate general principles which contribute to complex crystal structures, and deduce heuristics from which to choose candidate structures.

DFPP gives the enthalpy of various structures, the lowest enthalpy structure being stable. Under pressure the total enthalpy comprises a band structure term (the eigenvalues of non-interacting electrons moving in an effective field), an Ewald sum, pressure times volume, exchange correlation and Hartree energies.[1] The dependence on volume (Ω) is as follows: $\Omega^{-1/3}$ for the coulombic terms (Hartree, ion-ion, ion-electron), Ω^0 for the exchange correlation (neglecting “non-linear core corrections”), $\Omega^{-2/3}$ for kinetic energy. Thus under pressure materials become more free-electron like. We note two aspects of DFPP. Firstly, the fact that pseudopotentials work indicates that repulsion between core electrons can be neglected. Secondly, energy minimization in DFPP codes is hugely improved by *preconditioning*[2]: assuming that the contribution from a plane wave basis state is primarily its free-electron-like kinetic energy.

Two further effects are not explicit here: imperfect screening of ionic charge as ions approach closely and the FSBZ energy splitting from interaction between plane waves and ionic potentials[3]: $\Delta E = \pm \int_{\Omega} e^{i\mathbf{k}\cdot\mathbf{r}} V(\mathbf{q},\mathbf{r}) e^{i\mathbf{k}'\cdot\mathbf{r}} d^3\mathbf{r}$.

$V(\mathbf{q},\mathbf{r})$ depends on the scattering at $\mathbf{q}=\mathbf{k}+\mathbf{k}'$ which, for elements, is proportional to the X-ray diffraction. If \mathbf{k} falls near the Fermi level the state with increased energy is unoccupied, while the other is occupied. Thus FSBZ interaction gives a first order change in energy with crystal structure, while at other \mathbf{k} the energy gained and lost cancels. FSBZ effects scale as Ω^{-1} .

It is important to distinguish those terms which contribute most to the *total energy* from those which contribute to *energy differences between crystal structures*. The latter are the screened ion-ion potential and the perturbation of the free electrons from FSBZ interactions. Given its Ω^{-1} scaling with volume, FSBZ interaction may dominate at intermediate pressures with the $\exp(-\Omega^{1/3})$ dependence of imperfect screening being important at the highest pressures.

The central result of this paper will be the demonstration that the complex elemental crystal structures at intermediate pressures can be simply understood using NFE. This theory also gives a way of picking plausible trial structures for total energy calculation, and explains a number of observed properties. To ease comparison with experiment, we will refer to specific interactions between the FS and particular points in the BZ (diffraction peaks) rather than the equivalent[4] description in terms of BZ planes containing these points.

Under pressure, group I and II metals transform from simple structures, bcc and fcc, to complex structures. The striking similarity between the Cs-*oC84*, Rb-*oC52* and Li-*cI16* structures[5, 7, 8] is shown in Fig.2 and in the diffraction patterns (Fig.3): all are derivatives of bcc.

Complex phase stability in Rb and Cs[7, 8] has been attributed to *s* – *d* transfer of electrons allowing directional bonding and hence open structures. A strong justification for this was the now-discredited isostructural phase transition in Cs[7] which cannot be explained in a free-electron picture. In a localised basis picture *s* – *d* transfer transfer certainly exists, but offers no insight into the nature of the structures and cannot explain the Li-*cI16* structure(Fig.2) as there are no d-orbitals available to Li. DFPP calculations for *cI16* Li provide an ideal

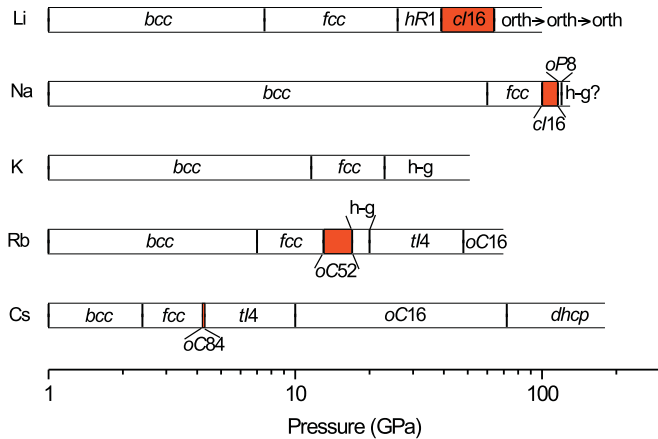


FIG. 1: High-pressure structural transition sequences for the alkali and alkaline earth elements[5, 6, 7, 8, 9, 10, 11, 12, 14, 15, 16]. The general pattern is similar, with low-Z materials having higher transition pressures. Intermediate structures are labelled in Pearson notation.

testbed for the alternate FSBZ picture (Fig.4): FSBZ effects scale strongly Ω^{-1} with reduced volume, causing increases in internal parameter x , (211) band gap opening and diffraction peak intensity. At very high pressure this is overcome by imperfect screening of ionic charges (exponential in $x\Omega^{1/3}$).

We have calculated the optimal value of x in $cI16$ Li using DFPP. Figure.4 shows variation of total energy with atomic position parameter x , for a range of volumes. Ewald and band structure contributions account for all the variation: for larger x the band structure energy is lowered, but the Ewald energy also increases and ultimately becomes dominant. Thus, the band structure energy is responsible for complex structure stability in Li and [5, 19, 20, 21]. the signature in powder diffraction is that one or more diffraction peaks approach k_F [34].

Precisely this signature exists in Cs and Rb Figure3, indicating similar physics. The interstitial atoms reduce volume per atom at the expense of splitting the the diffraction peak near to the Fermi level. In a real space picture the sequence of first increasing then decreasing interstitial number seems inexplicable. In the FSBZ picture, the Fermi surface is more easily deformed at large Z. For Li, the PV enthalpy gained from interstitials cannot compensate for loss of FSBZ interaction from peak splitting. Rb has FSBZ interactions with three of the four split peaks, while Cs deforms to touch all four.

This gives us the desired heuristic in the search for candidate “complex” structures for DFPP calculation: multiple strong diffraction peaks at the Fermi energy. It also suggests that a simple model of interatomic interactions in such materials should concentrate on a particular wavenumber in reciprocal space: a condition somewhat encapsulated long ago by Friedel oscillations.

With the FSBZ picture established for alkali metals, it is instructive to turn to other elements. Recently, com-

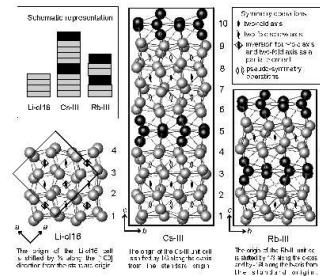


FIG. 2: Crystal structures of Li- $cI16$ (left) Cs-III (middle) and Rb-III (right) viewed along the $[100]$ axis, of the $C222_1$ unit cell. Interatomic distances up to 2.5\AA (Li), 4.7\AA (Cs) and 4.1\AA (Rb) are shown as solid lines. True symmetry operators normal to the plane of projection are shown by solid symbols, pseudo-symmetry operators by open symbols. The $cI16$ structure can be viewed as a simple distortion of body-centered cubic structure, in which each atom is shifted by x along the bcc $[111]$ directions [5]: in this projection we find 8-atom layers. For Cs-III and Rb-III[8] identical 8-atom layers exist[18] interspersed with 10-atom layers (black) which can be considered as 8-atom layers with (001) dumbbell interstitials inserted. Thus, the Cs- $oC84$ and Rb- $oC52$ structures are the same as Li- $cI16$ with density increased by interstitial atoms every fifth (Cs) or third (Rb) layer.

plex Li-type distorted bcc structures have been reported in gallium[17]. This extraordinary confluence of monovalent and trivalent materials would appear to contradict the FSBZ picture. However, fig.3 reveals the $(310)_{Li}$ -type diffraction peak just below the Fermi level. Such effects have also been observed in intermediate pressure phases of Group IV and III-V compounds[30].

In Rb, Ba and Sr a new principle emerges: In real space BaIV-type forms self-hosting “hotel” structures which can only be described using two interpenetrating crystal structures (the “host” and chains of “guests”)

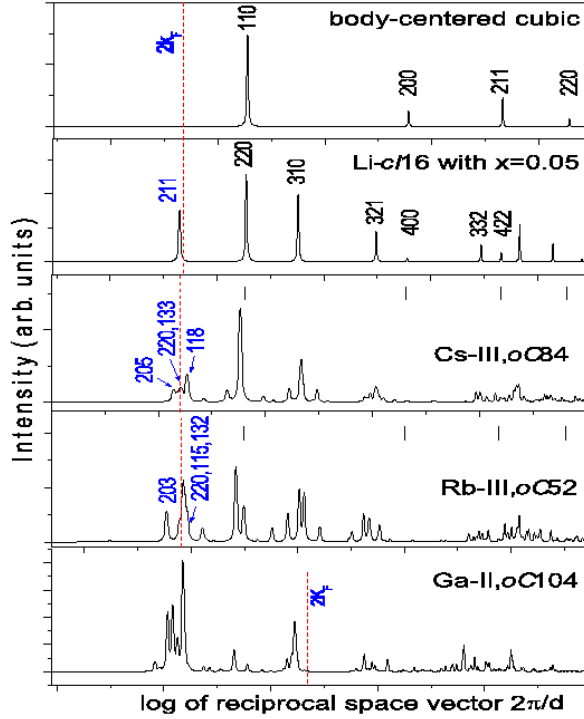


FIG. 3: Calculated diffraction patterns for bcc the complex structures of Li, Cs, Rb and Ga. The major effect of the *c/16* distortion in Li is to throw up a 211 peak just below the Fermi Vector[34], calculated assuming a free electron sphere to equate to $2\theta = 2 \sin^{-1}(\lambda \sqrt{3N/64\pi V})$

[9, 22, 23, 24]. The structures can be incommensurate, giving rise to two distinct Brillouin zones and the consequent additional possibilities for FSBZ interactions. Again their stabilities are well reproduced by DFPP[22].

Figure 5 shows their diffraction patterns - once again strong diffraction peaks lie near the Fermi level, and the FSBZ picture is dominant. Significantly, while in Ba and Sr there is interaction with the (201) guest, there is no guest reflection (with non-zero k_z) near the BZ in Rb. Thus FSBZ interaction order the positions of adjacent chains in Ba and Sr, but not in Rb: Indeed, inter-chain order is observed in Ba and Sr, but Rb undergoes a “melting” transition at low pressure. Similarly, the ratio between guest and host lattice parameters is pressure independent in Ba and Sr, (locked by the FS-(201)_g interaction), but pressure dependent in Rb, since no FSBZ effects fix the guest *c/a* ratio.

Other properties of the complex crystal structures in alkali metals relate to the FSBZ interpretation.

The resistivity in Li[26], rises tenfold between 40-120 GPa, corresponding to the *c/16* and other complex orthorhombic phases [5, 6]. Similar behavior is observed in Cs (4 GPa, the Cs-III phase) and Rb (10GPa, the Rb-II and Rb-III phases) [28]. Fig.4 shows that the FSBZ interaction which open pseudogaps at the Fermi level in Li-*c/16* giving much lower electron density at the Fermi

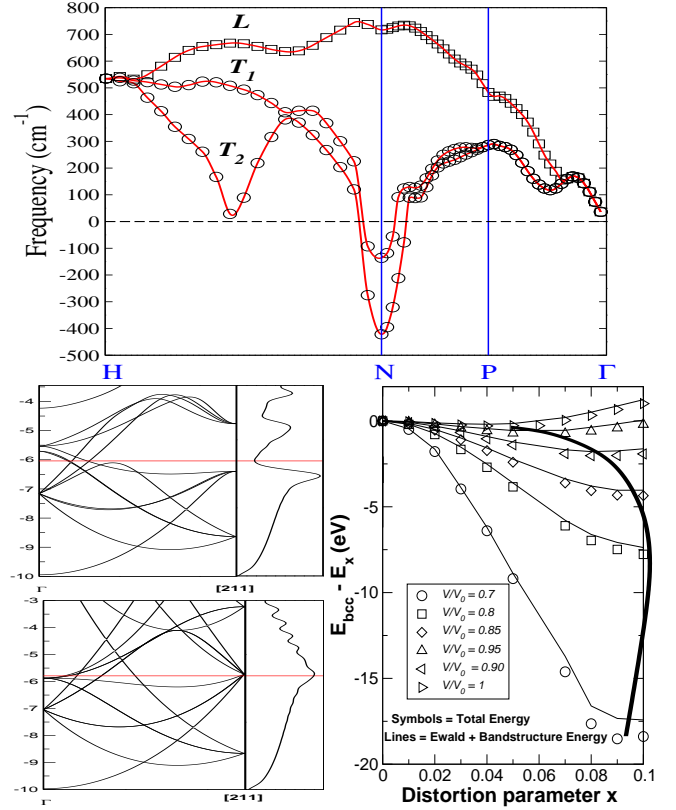


FIG. 4: Top: Ab initio calculation of phonon dispersion relation[33] showing dynamic instability for bcc-Li at 40GPa. Bottom: (right) Li-DFPP energy difference between bcc and *c/16* for various *x* over a range of volumes ($V_0 = 146.4A^3$, the volume at which *c/16* is first observed). The structure is stable between 42-50 GPa $V/V_0=1-0.85$. Symbols are total energy, lines are Ewald and bandstructure only, showing that the Hartree and exchange-correlation contributions are negligible. The thick line indicates the optimum value of *x* at each volume. (left) Band structures along the $[2x,x,x]$ direction for $V_0, x=0$ (lower panel) and $x=0.05$ (upper panel) showing the opening of a pseudogap due to FSBZ interactions: the surface touches the 24 (211) BZ planes. Elsewhere in the BZ bcc and *c/16* band structures are similar.

level than in fcc and bcc phases.

Superconductivity arises from coupling of electrons to low frequency vibrational modes; we have not performed detailed calculations, but complex phases tend to exhibit superconductivity through the the low frequency phonons associated with FSBZ effects, and phasons of incommensurate phases. Superconductivity is observed in complex structures of Li *c/16* phase[5], Cs, Ba, Sr and Ga. In contrast superconductivity is not detected in Rb up to pressures of 21 GPa[29], where the weak non-FSBZ interchain coupling melts the phason mode.

Projection of our wavefunctions onto atomic orbitals shows increased *d* character with pressure, however, we have shown that the concept of FSBZ interactions provides a better simple description for the “complex”

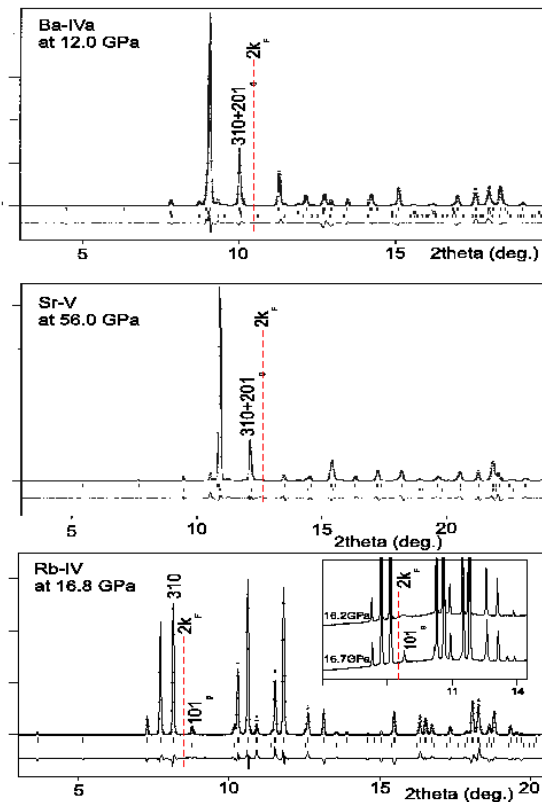


FIG. 5: Calculated diffraction patterns for hotel structures of Ba-IV, Sr-V and Rb-IV. The tick marks show whether the reflection is from host (upper) or guest (lower) lattice. The insets show how the Brillouin zone maintains contact with the Fermi surface.

phases observed under pressure than does $s-d$ transfer. A simple heuristic for stable phases is the existence of strong diffraction peaks just below the free-electron Fermi vector[34]. Monovalent elements achieve this by distortion of bcc with FSBZ at (211) peaks; divalent materials form host-guest structures with two Brillouin Zones and trivalent gallium adopts distorted-bcc structures with FSBZ at (310) peaks. Unlike $s-d$ transfer, the theory also accounts qualitatively for the chain-melting and pressure sensitivity of c/a in rubidium, pressure independence of c/a ratio in Ba and Sr, the increased superconductivity transition temperature in complex phases, and the similarity of Li with other group-1 elements under pressure.

We acknowledge discussions with M.I.McMahon, R.J.Nelmes and V.Degtyareva. Calculations were done using the VASP and PWscf packages[35]

- [1] W.Kohn and L.J.Sham, Phys. Rev.**140**, 1133A (1965).
- [2] M.C. Payne, M.P. Teter, D.C. Allan, T.A. Arias and J.D. Joannopoulos.*Rev. Mod. Phys.*, **64** 1046 (1992).
- [3] N.F.Mott and H.Jones *The Theory of Metals and Alloys* Clarendon Press, Oxford (1936)
- [4] Strictly, FSBZ energy from second order perturbation theory requires an integral between pairs of occupied and

unoccupied orbitals in adjacent BZs. This integral is complicated enough to obscure the simple picture, yet quantitatively less accurate than DFPP calculation - since its value varies with the interaction at the diffraction peak, we use the latter for qualitative discussion.

- [5] M. Hanfland, K. Syassen, N.E. Christensen, and D.L. Novikov, Nature **408**, 174 (2000).
- [6] M.Hanfland, I.Loa, K.Syassen Phys. Rev. B **65** 184109 (2002); *ibid.* Unpublished work
- [7] M.I. McMahon, R.J. Nelmes, and S. Rekhi, Phys. Rev. Lett. **87**, 255502 (2001).
- [8] R.J. Nelmes, M.I. McMahon, J.S. Loveday, and S. Rekhi, Phys. Rev.Lett. **88**, 155503 (2002).
- [9] M.I. McMahon, S. Rekhi, and R.J. Nelmes, Phys. Rev. Lett. **87**, 055501 (2001). U. Schwarz, A. Grzechnik, K. Syassen, I. Loa, and M. Hanfland, Phys.Rev.Lett. **83**, 4085-4088 (1999).
- [10] H.Olijnyk, W.B.Holzappel, Phys.Lett.**99A**, 381 (1983).
- [11] K. Takemura, S. Minomura, and O. Shimomura, Phys. Rev. Lett. **49**, 1772 (1982).
- [12] U. Schwarz, K. Syassen, A. Grzechnik, and M. Hanfland, Solid State Commun. **112**, 319 (1999).
- [13] U. Schwarz, K. Takemura, M. Hanfland, and K. Syassen, Phys.Rev.Lett. **81**, 2711 (1998).
- [14] K. Takemura, N.E. Christensen, D. L. Novikov, K. Syassen, U. Schwarz, and M. Hanfland, Phys. Rev. B **61**, 14399 (2000).
- [15] M. Winzenick, V. Vijayakumar, and W.B. Holzappel, Phys. Rev. B **50**, 12381-12385 (1994); M. Winzenick, PhD thesis, Paderborn, Germany (1996).
- [16] M.I. McMahon, private communication.
- [17] O.Degtyareva, M.I.McMahon D.R.Allan and R.J.Nelmes, submitted.
- [18] Layers are inclined at about $\pm 35^\circ$ to the conventional b -axis [8]. The angle of 35° originates as the angle between bcc planes (110) and (111); it does not change in the bcc-CII6 transformation.
- [19] F. Siringo, R. Pucci and G.G.N. Amgilella, High Press. Research **15**, 255 (1997).
- [20] J.B. Neaton and N.W. Ashcroft, Nature **400**, 141 (1999).
- [21] J.B. Neaton and N.W. Ashcroft, Phys.Rev.Lett, **86**, 2830 (2001).
- [22] S.K.Reed, G.J.Ackland Phys.Rev.Lett, **84**, 5580, (2000)
- [23] McMahon MI, Bovornratanaraks T, Allan DR, Belmonte SA and Nelmes RJ Phys Rev B **61** 3135 (2000)
- [24] Nelmes RJ, Allan DR, McMahon MI, Belmonte SA, Phys Rev Lett **83** 4081 (1999)
- [25] N.W. Ashcroft, Acta Cryst. A**58**, C61 (2002).
- [26] V.E. Fortov, V.V. Yakushev, K.L. Kagan, I.V. Lomonosov, V.I. Postnov, and T.I. Yakusheva, JETP Letters **70**, 628 (1999); JETP Letters **74**, 418 (2001).
- [27] N.E. Christensen and D.L. Novikov, Phys. Rev. Lett. **86**, 1861 (2001).
- [28] P.W. Bridgman, Proc. Am. Acad. Arts Sci. **81**, 165 (1952). R.A. Stager and H.G. Drickamer, Phys. Rev. Lett. **12**, 19 (1964).
- [29] K.Shimizu, H.Ishikawa, D.Takao, T.Yagi and K.Amaya, Nature **419**, 597 (2002); V.V.Struzhkin, M.I.Eremets, W.Gan, H.Mao, and R.J.Hemley, Science **298**, 1213 (2002); J.Wittig, Phys. Rev. Lett. **24**, 812 (1970); K.Ulrich and J.Wittig, Bull. Amer. Phys. Soc. **25**, 433 (1980); W.Buckel and W.Gey, Z. Phys. **176**, 336 (1963).
- [30] G.J.Ackland, Rep.Prog.Physics **64**, 483-517 (2001)
- [31] V.F.Degtyareva, Phys.Rev.B **62** 9 (2000)

- [32] O.Degtyareva, V.F.Degtyareva, F.Porsch and W.B.Holtzapfel J.Phys.CM **13** 7295 (2001)
- [33] G.J.Ackland, M.C.Warren and S.J.Clark, J.Phys.CM **9**, 7861 (1997).
- [34] In DFPP some high-k components are mixed into low energy states, so the free-electron-like states at E_F will have wavevectors below the free electron k_F . For maximum BZFS effect k_F should lie just above the relevant diffraction peak. $s - d$ transfer arguments give a similar picture by assuming fewer free electrons.
- [35] S.Baroni, A.DalCorso, S.deGironcoli, and P.Giannozzi, www.pwscf.org ; G.Kresse, cms.mpi.univie.ac.at/vasp/